Polym. Bull. (2012) 68:647–665
DOI 10.1007/s00289-011-0562-4

ORIGINAL PAPER

Copper-mediated ATRP of MMA in DMSO from unprotected dextran macroinitiators

Ludovic Dupayage · Cécile Nouvel · Jean-Luc Six

Received: 14 May 2010 / Revised: 20 June 2011 / Accepted: 21 June 2011 /
Published online: 29 June 2011
© Springer-Verlag 2011

Abstract To easily perform atom transfer radical polymerization (ATRP) of methyl methacrylate (MMA) in homogeneous medium from unprotected polysaccharidic macroinitiators, the ATRP of MMA carried out in dimethylsulfoxide has been firstly reinvestigated using Cu(I)Br as metal catalyst and ethyl 2-bromoisobutyrate as initiator. Two ligands, 2,2′-bipyridyne (Bpy) and *N*-(*n*-propyl)-2-pyridylmethanimine (*n*-Pr-PMI), have been compared, as well as the addition of $Cu(II)Br_2$ (10 molar % relative to Cu(I)Br) or the adjustment of experimental temperature (from 30 to 60 °C). Appropriate conditions were founded for both ligands to achieve a controlled ATRP. Bpy giving far much faster polymerization compared to *n*-Pr-PMI, *n*-Pr-MI was preferred as ligand for accurate tuning of the conversion. Experimental procedure was then applied to unprotected macroinitiators based on dextran to obtain amphiphilic poly(methyl methacrylate) grafted dextran. While homopolymerization was controlled in these conditions, parameters have to be adjusted for the hydrophilic unprotected macroinitiators to prevent gel formation and control ATRP.

Keywords ATRP · DMSO · Dextran · Graft copolymers · Amphiphiles · Biopolymers

Introduction

Controlled radical polymerizations are powerful and easy tools for preparation of many well-defined polymers with precisely controlled architecture [1–3]. Atom transfer radical polymerization (ATRP) is one of the best and easiest among such radical processes for the design of a large number of macromolecular architectures

L. Dupayage · C. Nouvel (✉) · J.-L. Six
Laboratoire de Chimie Physique Macromoléculaire, UMR 7568 CNRS, Nancy University,
1 rue Grandville, BP 20451, 54001 Nancy Cedex, France
e-mail: Cecile.Nouvel@ensic.inpl-nancy.fr

with controlled parameters [4–6]. This method proceeds via a reversible homolytic cleavage of an activated carbon halogen bond [2]. Many papers have already described its mechanisms as well as the influence of various parameters such as monomer, initiator, metal complexes, ligand or solvent on the polymerization process. The nature of the solvent plays a crucial role in terms of overall rate, molecular weight control, and initiator efficiency. Generally, cooper catalysts have been the most used for ATRP of methyl methacrylate (MMA) in bulk, in solution, or in dispersed medium. A large variety of non polar solvents (toluene [7, 8], xylene [8]) and more or less polar ones (diphenylether [9, 10], acetonitrile [11], ethylene glycol [12], *N*,*N*-dimethylformamide (DMF) [11, 13], dimethylsulfoxide (DMSO) [11],water/DMF mixture [14], ethyl acetate [15]) have already been tested for MMA. Usually, ATRP in polar solvent exhibited higher polymerization rate compared to those carried out in non-polar ones. But the main advantage of these polar solvents is their ability to solubilize hydrophilic initiators, either low-molecular weight sugar-based [12] compounds or polysaccharides derivatives [16, 17], poly(ethylene oxide) derivatives [18], or water-soluble polyvinyl derivatives such as poly(potassium 3-sulfopropyl methacrylate) [14].

Recently comb-like glycopolymers with well-defined architecture were developed in our laboratory by the "grafting from" strategy [19, 20] to be used as biocompatible and biodegradable surfactants [21, 22] such as polylactide-grafted dextran (Dex-g-PLA). Lately, we developed the same strategy to synthesize poly(methyl methacrylate)-grafted dextran copolymers (Dex-g-PMMA) using ATRP as controlled polymerization [17]. In this previous study, amphiphilic glycopolymers were obtained thanks to a four-step synthesis using a partially protected dextran macroinitiator DexAcBr (Scheme 1) soluble in a variety of solvent. To both obtain straightforwardly Dex-g-PMMA and to fully study macromolecular engineering opportunities, another synthetic macroinitiator DexBr was developed by direct introduction of initiator group in dimethylsulfoxide (Scheme 1). But the solubility of the DexBr macroinitiator used in this study is very similar to initial dextran and limits the number of solvent available for ATRP of MMA essentially to DMSO. Indeed, these problems of solubility have considerably hampered extensive use of ATRP from unprotected polysaccharide macroinitiators and consequently only a few works have reported homogeneous ATRP of various vinylic monomers from these derivatives (cellulose [16, 23–25], pullulan [14], or dextran [14, 26] macroinitiators). Although solubility is very depending on the polysaccharide, the choice of solvent used for ATRP is also based on monomer polarity. If MMA has already being polymerized from cellulose macroinitiators in DMF [24] or in ionic liquid [25] or from pullulan in DMF/water (80/20 v/v) [14], it was never polymerized from any polysaccharide in DMSO.

Unprotected synthesis of Dex-g-PMMAs having never been published so far, our final objectives are to perform it homogeneously in DMSO where both dextran and PMMA are soluble. To optimize the conditions for macromolecular engineering from DexBr macroinitiator, we firstly decided to reinvestigate the behavior of methyl methacrylate ATRP in DMSO with EBiBr as model initiator and to test afterward polymerization from macroinitiators. To our knowledge, only two publications to date are reporting ATRP of MMA in DMSO [11, 27]. These polymerizations were carried out using Cu(I)Br as metal catalyst, ethyl

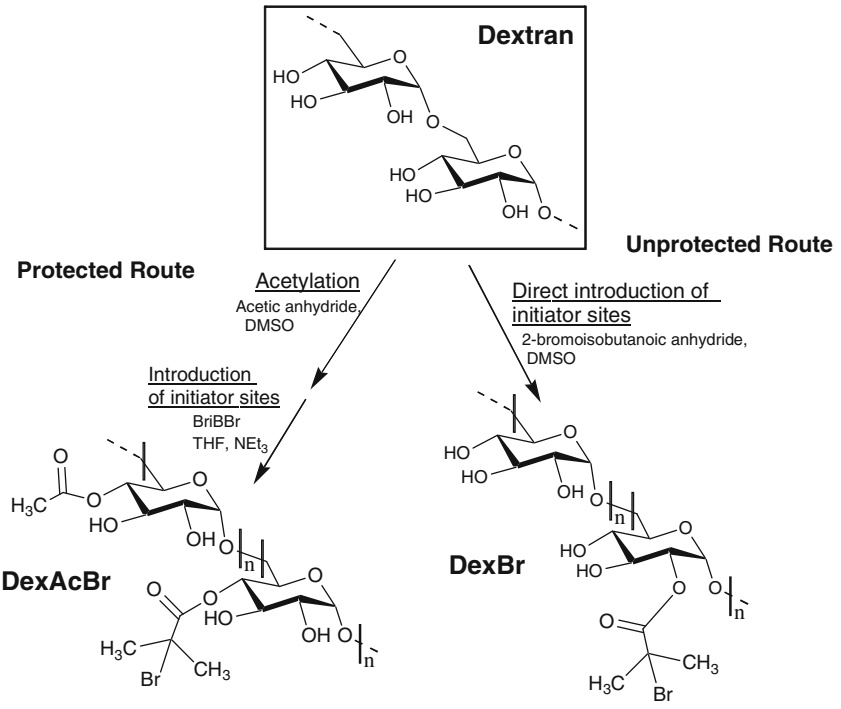

Scheme 1 Synthesis of both macroinitiators derivated from dextran: protected route versus unprotected route

2-bromoisobutyrate (EBiBr) as model initiator and classical Schiff bases ligands like *n*-Pr-PMI [27] or a new diimine base (bis(2-pyridinal)ethylenediimine) [11]. The best results in term of kinetics plots, molecular weights, and polydispersities have been obtained by Haddleton's group [27]. Starting from theses experimental conditions, our first results were founded slightly different. To improve the control of the homopolymerization, several parameters were studied such as initial adding of $Cu(II)Br_2$ or decreasing polymerization temperature. Finally, another ligand (Bpy) was compared to *n*-Pr-PMI to complete the first study. In a second time, the chosen experimental conditions issued from the model study were successfully applied to DexAcBr macroiniators but need to be adapted in the case of DexBr, due to very high-polymerization rate.

Experimental section

Materials

N-propylamine (Aldrich 99%), pyridine-2-carboxaldehyde (Aldrich 99%), 2-bromoisobutyryl bromide (B^iBB), 2,2′-dimethylaminopyridine (DMAP), diethyl ether (Fluka 99.5%), magnesium sulfate (VWR), and methyl acrylate (MA, Aldrich 99%) were all used as received. The *N*-(*n*-propyl)-2-pyridylmethanimine (*n*-Pr-PMI) [8]

and 2-Bromoisobutyryl anhydride [28] were prepared using a literature procedure with slight modifications. Ethyl 2-bromoisobutyrate (EBiBr), copper bromide (Cu(I)Br), 2,2′-bipyridyne (Bpy), and anisole were obtained from Aldrich, while copper dibromide (Cu(II)Br_2) was obtained from Fluka. All of those were used without further purification. Methyl methacrylate (MMA, Aldrich 99%) and dimethylsulfoxide (DMSO, Fischer scientific 99%) were vacuum distilled from CaH_2 and stored under nitrogen atmosphere. Pyridine (Aldrich) was dried over BaO and filtered before use.

Synthesis of dextran macroinitiators

Protected macroinitiators DexAcτ_{Ac}Brτ_{Br}

Protected macroinitiators DexAcτ_{Ac}Brτ_{Br} were synthesized in two steps as previously reported [17]. In the first step, the dextran OH functions were partially acetylated. The second step consisted in linking initiator groups by reaction of B^iBB with the unprotected OH functions. τ is the modification yield (that is, the number of acetate (τ_{Ac}) or of initiator groups (τ_{Br}) for 100 OH of the initial dextran).

Unprotected macroinitiator DexBrτ_{Br}

Firstly, 1 g of dextran (6.2 mmol of glucosidic units, 18.5 mmol of OH) was dissolved in DMSO (18 mL). 0.11 g of DMAP (0.05 mol per mol of OH) was dissolved in 4.5 mL of dried pyridine (3 mol per mol of OH), then added to the dextran solution. To obtain a dextran derivative with τ_{Br} of 20%, 2.4 g of 2-bromoisobutyryl anhydride (7.6 mmol) was then slowly introduced at 0 °C during half an hour, and the reaction was left at room temperature for 20 h. The polymer was precipitated twice in acetone, and the product was filtrated, washed, and dried at 50 °C under vacuum during 24 h. τ_{Br} (%) was evaluated by ^{1}H NMR in DMSO-d_6 using Eq. 1 where A_{Br} is the area of the singlet around 1.9 ppm, which is characteristic of methyl protons from the initiator group. As previously in the case of DexAcBr [17], the global area from 4 to 5.7 ppm (called $A_{4\rightarrow5.7}$), corresponded to four protons (the coupling of the initiator group on any OH induced the shift of the glucosidic H supported by the same C).

$$\tau_{Br}\ (\%) = \left(\frac{A_{Br}}{A_{4\rightarrow5.7}}\right) \times \frac{4 \times 100}{18}. \qquad (1)$$

ATRP of MMA

The model initiator

In a typical experiment, 14 mL of MMA (0.13 mol), 18 mL of DMSO, and 1.4 mL of anisole (0.01 mol, used as NMR reference) have been introduced in a reactor under nitrogen atmosphere. Next, Cu(I)Br (193 mg, 1.35 mmol) and sometimes Cu(II)Br_2 (30 mg, 0.13 mmol) have been added in addition with appropriated

quantities of ligand (Bpy or *n*-Pr-PMI). After 10 min of stirring, the reaction mixture was degassed by three freeze–pump–thaw cycles, and the reactor was then immersed in a thermostated oil bath at the reaction temperature (60 or 30 °C). The initial MMA/anisole ratio ($[MMA]_0/[Anisole]_0$) was estimated by ^{1}H NMR analysis of an immediate aliquot. Polymerization was started by adding 0.2 mL of EBiBr (1.35 mmol). To follow the conversion yield and the evolution of molar masses, samples have been taken at different times throughout the reaction. Monomer conversion was determined by ^{1}H NMR in $CDCl_3$ using Eq. 2 from the area of both singlet of MMA methylene protons (A_{MMA}, at 5.5 and 6 ppm) and that of some anisole protons ($A_{Anisole}$, 3H at 6.8 ppm).

$$\text{Conversion } (\%) = 1 - \frac{3 \times A_{MMA}}{2 \times A_{Anisole}} \times \frac{[Anisole]_0}{[MMA]_0} \times 100. \quad (2)$$

Catalyst residues were removed by passing through a short silica column using THF as eluent. Crude PMMA has been precipitated twice from petroleum ether and dried overnight at 50 °C under vacuum. Purified product was then analyzed both by SEC-MALLS using THF as eluent and by ^{1}H NMR in $CDCl_3$.

The DexAcBr macroinitiator

Experimental protocol is already published [17]. For example, in the case of $DexAc_{71}Br_6$, typical experimental conditions were as follows: $[MMA]_0 = 4$ M, $[Anisole]_0 = 0.4$ M, $[MMA]_0/[Br]_0/[n\text{-Pr-PMI}]_0/[Cu(I)Br]_0/[Cu(II)Br_2]_0 = 100/1/2/1/0.1$ (molar ratio), where $[Br]_0$ is the initial concentration of bromide (here $[\text{initiator group}]_0$). To follow the conversion yield and the evolution of molar masses, samples have been taken at different times throughout the reaction. Monomer conversion was determined by ^{1}H NMR in $CDCl_3$ using previous Eq. 2. For each sample, catalyst residues were removed as previously described. Crude sample was purified by precipitation twice by petroleum ether and then dried overnight at 50 °C under vacuum. The purified product was called DexAc-g-PMMA.

The DexBr macroinitiator

DexBr has been dissolved in DMSO. Then predetermined amounts of *n*-Pr-PMI, Cu(I)Br, and finally $Cu(II)Br_2$ were successively introduced in the reactor, while a solution of anisole (0.1 M) in MMA was prepared separately. Each mixture was degassed by three freeze–pump–thaw cycles after a 10-min stirring, and then the reactor was heated at convenient temperature (that is 45 or 60 °C). Afterward an appropriate volume of the anisole solution (0.4 M in MMA) was transferred in the reactor with a canula. At this time, the polymerization was started. For example, in the case of $DexBr_{4.3}$, typical experimental conditions were as follows: 45 °C, $[MMA]_0 = 4$ M, $[Anisole]_0 = 0.4$ M, $[MMA]_0/[Br]_0/[n\text{-Pr-PMI}]_0/[Cu(I)Br]_0/[Cu(II)Br_2]_0 = 100/1/2/1/0.1$ (molar ratio), where $[Br]_0$ is the initial concentration of bromide (here $[\text{initiator group}]_0$). The evolutions of conversion yield and of molar masses were followed as above. Catalyst residues were removed as previously

described. Crude sample was purified by precipitation twice by petroleum ether and dried overnight at 50 °C under vacuum. The purified product was called Dex-g-PMMA.

Cleavage of the PMMA grafts from dextran backbone

As previously reported [17], the dextran backbone of DexAc-g-PMMA or of Dex-g-PMMA (500 mg) was completely degraded using 60 mL of THF/(1 M KOH–MeOH) (2/1 v/v) under stirring at room temperature for 72 h in order to study the PMMA grafts subsequently. The recovered mixture was then neutralized with 1 M HCl. After evaporation of THF and methanol, PMMA chains were solubilized in toluene, and the solution was filtered in order to remove KCl. PMMA was recovered by precipitation with petroleum ether filtration and was then dried overnight at 50 °C under vacuum. The polymers were analyzed by ^{1}H NMR in DMSO-d_6 to prove the absence of the dextran backbone. The molar masses of PMMA chains and their distribution were then characterized by SEC-MALLS in THF. We have already reported [17] that under these hard basic conditions, no degradation of PMMA chain was observed, and the stability of the methyl ester of each monomer unit was ascertained by ^{1}H NMR analyses.

Characterization

^{1}H NMR spectra were recorded on a Bruker Avance 300 apparatus (300, 13 MHz, 25 °C) in $CDCl_3$. Size exclusion chromatography coupled to multi-angle laser light scattering (SEC-MALLS) was performed at room temperature using a Merck HPLC pump (L-6200A) equipped with a degazer, three PLgel 5 μm columns [100 Å, 300 × 7.5 mm; 1000 Å, 300 × 7.5 mm and guard columns, 50 × 7.5 mm (Polymer laboratories)]. THF was used as eluent, at elution rate 0.7 mL/min. Two detectors were used online: a Multi-Angle Light Scattering detector (MALLS) and differential refractometry (Merck RI-71). A refractive index increment (dn/dc) of 0.087 was used.

Results and discussion

ATRP of MMA in DMSO

Model study

To easily perform ATRP in homogeneous medium from hydrophilic dextran macroinitiators, we firstly tried to achieve successful ATRP of MMA in DMSO, relying on Haddleton's group results [27]. First assays were conducted at 60 °C with EBiBr as initiator and Cu(I)Br as metal catalyst in similar conditions to the previous report [27] with *N*-(*n*-propyl)-2-pyridylmethanimine (*n*-Pr-PMI) as ligand (Fig. 1): the initial molar ratio of $[MMA]_0/[EBiBr]_0/[Cu(I)Br]_0/[n\text{-Pr-PMI}]_0$ was 100/1/1/2

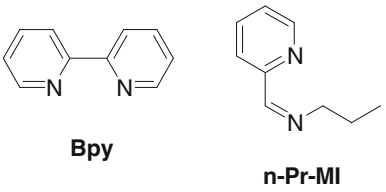

Fig. 1 Structures of the used ligands

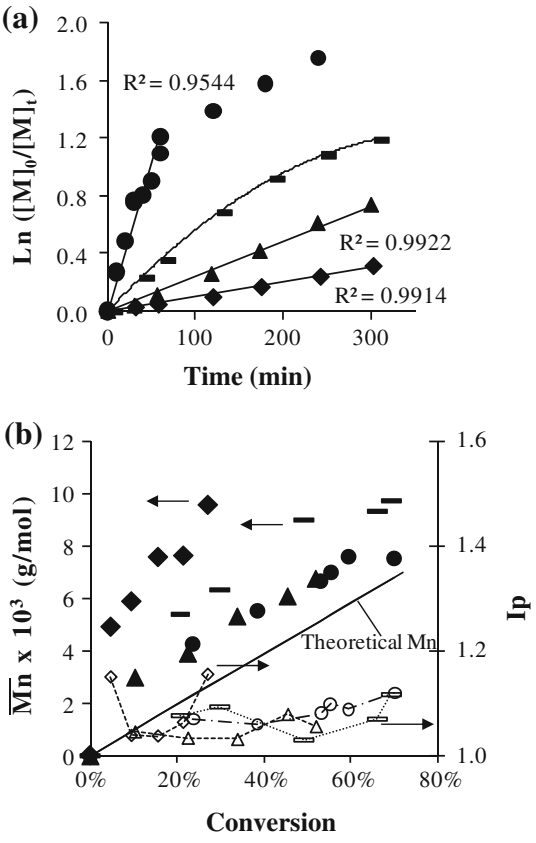

Fig. 2 Polymerization of MMA in DMSO using EBiBr as initiator at 60° with the following conditions : Anisole/MMA = 1/10 (v:v); $[MMA]_0$ = 4 mol/L; $[MMA]_0/[EBiBr]_0/[Cu(I)Br]_0/[L]_0$ = 100/1/1/2 (molar ratio). *n*-Pr-PMI or Bpy as ligand was noted L. **a** Evolution of $\ln([M]_0/[M]_t)$ versus time. **b** Evolutions of experimental $\overline{M_n}$ (*full symbols*), of theoretical $\overline{M_n}$ (*plain line*), and of polydispersity index I_P (*open symbols*, *dotted line*) versus conversion. With *n*-Pr-PMI, *filled rectangle*: 60 °C, $[Cu(II)Br_2]_0$ = 0; *filled triangle*: 60 °C, $[Cu(II)Br_2]_0/[Cu(I)Br]_0$ = 0,1 (molar ratio); *filled diamond*: 30 °C, $[Cu(II)Br_2]_0$ = 0. With Bpy, *filled circle*: 60 °C, $[Cu(II)Br_2]_0/[Cu(I)Br]_0$ = 0,1 (molar ratio)

with $[MMA]_0$ equal to 4 mol/L, while the ratio and $[MMA]_0$ were equal to 127/1/1/2 and 4.7 mol/L, respectively, in the previous study [27]. Anisole was added as internal standard ($[Anisole]_0/[MMA]_0$ = 1/10 (v:v)). As depicted in Fig. 2a, the observed kinetics was fast, and more than 70% of the MMA was polymerized in only 5 h. Indeed, this rapid polymerization comes both from the polarity of the solvent modifying the stability of the polymerization intermediates and from changes in the catalyst structure due to competitive complexation of ligand and DMSO onto the metal catalyst [27]. Both factors encourage the activation of halogen species into active ones and increase reaction rate.

The kinetics semilogarithmic plot in Fig. 2a showed significant downward curvature after around 50% of conversion indicating that irreversible termination reactions occurred. These secondary reactions induced a nonlinear evolution of the molecular weight (Fig. 2b) even if polydispersity indexes remained narrow ($M_w/M_n = 1.05–1.2$). Furthermore, molecular weight values were higher than the predicted ones, which could result either from partial initiation efficiency or the occurrence of combination terminations. But, such values of M_n can not only be explained from termination as PMMA active chains terminate preferentially by disproportionation compared to combination (67 and 73% of disproportionation at 25 and 60 °C, respectively). As a consequence, these differences between experimental and theoretical M_n should necessary come from no-quantitative initiator efficiency.

The deviation from linearity of the kinetics semilogarithmic curve may also come from the existence of "self-regulation" caused by the so-called "persistent radical effect" inducing termination reactions. As stated before [29], irreversible termination occurs at the beginning of the polymerization in the absence of deactivating species (here Cu(II)Br_2) at this initial stage. These terminations induce an increase of the deactivating species concentration until a sufficient value to prevent termination reactions. Therefore, in case of "persistent radical effect," the evolution of $\ln\left(\frac{[M]_0}{[M]_t}\right)$ is linear versus $t^{2/3}$ instead of t (see Eqs. 3 vs. 4) [7]. As plotted in the Fig. 3, the evolution of $\ln\left(\frac{[M]_0}{[M]_t}\right)$ versus $t^{2/3}$ was linear under our conditions. This attested the influence of persistent radical effect.

$$\ln\left(\frac{[M]_0}{[M]_t}\right) = \frac{3}{2}k_p([\mathrm{RX}]_0[\mathrm{Cu(I)}]_0)^{1/3}\left(\frac{K_{\mathrm{eq}}}{3k_t}\right)^{1/3}t^{2/3} = k_{\mathrm{Fischer}} \times t^{2/3} \qquad (3)$$

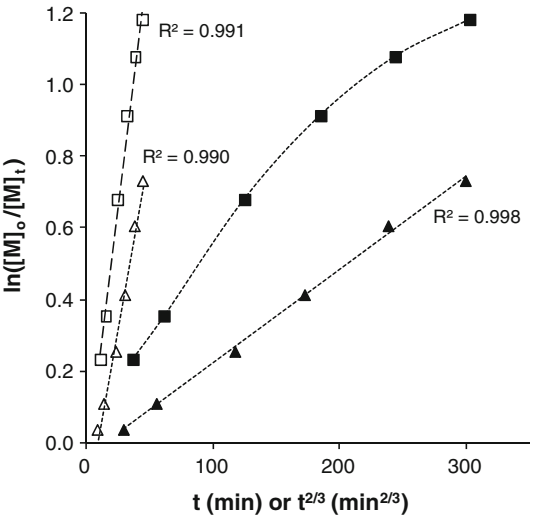

Fig. 3 Polymerization of MMA in DMSO using EBiBr as initiator, *n*-Pr-PMI as ligand at 60 °C with and without initial addition of $CuBr_2$. Anisole/MMA = 1/10 (v:v); $[MMA]_0$ = 4 mol/L; $[MMA]_0/[EBiBr]_0/[Cu(I)Br]_0/[n\text{-Pr-PMI}]_0$ = 100/1/1/2 (molar ratio). Evolution of $\ln([M]_0/[M_t])$ versus t (*full symbols*) or versus $t^{2/3}$ (*open symbols*). *Full square*: $[Cu(II)Br_2]_0 = 0$; *full triangle*: $[Cu(II)Br_2]_0/[Cu(I)Br]_0$ = 0,1 (molar ratio)

$$\ln\left(\frac{[M]_0}{[M]_t}\right) = k_p K_{eq} \frac{[RX]_0 \cdot [Cu(I)]_0}{[Cu(II)]_0} t = k_{app} \times t \quad (4)$$

To resume, termination reactions due to persistent radical effect restrain control over the polymerization in these conditions. Therefore, we studied the effect of various parameters such as adding of $Cu(II)Br_2$ in the initial mixture or decreasing polymerization temperature, in order to prevent such secondary reactions.

Initial amount of Cu(II)Br$_2$ and temperature effects

On the one hand, $Cu(II)Br_2$ was added in the initial state of the polymerization to confirm the former "persistent radical effect" hypothesis. The presence of initial amount of $Cu(II)Br_2$ reduces indeed the radical concentration by displacement of the activation/deactivation equilibrium and consequently decreases the global reaction rate. If the initial concentration of $Cu(II)Br_2$ is sufficient, this prevents irreversible termination reactions, which usually occur at the beginning of the polymerization without $Cu(II)Br_2$, and it ensures the control of the polymer growth. On the other hand, decreasing the polymerization temperature will also reduce the radical concentration and the polymerization rate. The influence of these two parameters (addition of $Cu(II)Br_2$ and temperature) is depicted in Fig. 2 for comparison with the previous ATRP. Experiments were conducted with or without initial addition of $Cu(II)Br_2$ at 60 °C, while a third one was carried out without Cu(II) at 30 °C. The polymerization control was improved in both cases (decreasing temperature and adding Cu(II)) and both kinetics experiments showed a linear semilogarithmic plot until 5 h of polymerization (Fig. 2a). The reaction was nevertheless faster at 60 °C with $Cu(II)Br_2$ compared to 30 °C without Cu(II). Thus, conversion after 5 h of polymerization is only 27% for the kinetics at 30 °C against 52% at 60 °C with $Cu(II)Br_2$. Our results with $Cu(II)Br_2$ appeared to be very similar to the kinetics already reported [27], even though Haddleton group's has purified their catalyst according to Keller and Wycoff [30].

But one remaining question was whether the amount of $Cu(II)Br_2$ added at the beginning was not too high, thus inducing slower polymerization rate. Previous studies have already been made to evaluate the adequate amount of $Cu(II)Br_2$ to add at the beginning of the polymerization [7]. This minimal amount, other called threshold concentration ($[Cu(II)Br_2]_{threshold}$), is the lowest one that enable a linear kinetic plot of $\ln\left(\frac{[M]_0}{[M]_t}\right)$ versus time and versus $t^{2/3}$, while the concentrations in Cu(II) and Cu(I) species remain constant all through the polymerization. However, if initial $Cu(II)Br_2$ concentration is lower than ($[Cu(II)Br_2]_{threshold}$), $\ln\left(\frac{[M]_0}{[M]_t}\right)$ is only linear versus $t^{2/3}$, while $\ln\left(\frac{[M]_0}{[M]_t}\right)$ is only linear versus time when initial concentration is higher than ($[Cu(II)Br_2]_{threshold}$). Therefore, Fischer and coworkers have estimated a threshold concentration for a $Cu(II)Br_2$/Cu(I)Br molar ratio of 10%, in case of the ATRP of MMA in toluene at 90 °C using 2-hydroxyethyl-2-bromoisobutyrate as initiator [7]. In our case, with 10% $Cu(II)Br_2$/Cu(I)Br molar ratio, $\ln\left(\frac{[M]_0}{[M]_t}\right)$ was linear versus both t and $t^{2/3}$ as shown in Fig. 3. On the reverse, when no $Cu(II)Br_2$ was

initially added only $\ln\left(\frac{[M]_0}{[M]_t}\right)$ versus $t^{2/3}$ was linear. Thus, the initial concentration of Cu(II)Br_2 (10 molar % per Cu(I)Br) we added matches the ($[Cu(II)Br_2]_{threshold}$) in our study and should not be decreased to maintain the ATRP control.

SEC curves of two experiments (60 °C with Cu(II)Br_2 compared to 30 °C without Cu(II)) showed monomodal distribution all through the polymerization. Moreover, the evolution of molecular weights versus conversion of these two kinetics experiments was plotted comparatively to the previous one at 60 °C without Cu(II)Br_2 (Fig. 2b). The plot of M_n versus conversion was not linear for the kinetics at 30 °C. This non-linearity, in addition with the slightly increase of the polydispersity indexes with conversion, indicated the occurrence of non-negligible transfer reactions during the polymerization at 30 °C. To the reverse, the experiment at 60 °C with initial Cu(II)Br_2 showed an almost linear increase of molecular weights with low-polydispersity indexes, which proved the control over the polymerization until more than 50% of conversion.

Moreover, the experimental values of molecular weight were higher than the predicted ones: the difference between experimental and theoretical values was attributed to the initiation efficiency Eff (around 67%). This no-quantitative initiation efficiency is not really surprising as EBiBr initiator is known to have efficiency values lower than 1 when used for ATRP of MMA. Since the $\ln\left(\frac{[M]_0}{[M]_t}\right)$ versus time plot is linear, low-initiator efficiency must be caused by consumption of some initiator due to side reactions at the first stage of the reaction [9, 31]. Those could have originated from primary coupling of radical issued from the initiator and/or from the more labile C–Br bond end groups at the beginning of the reaction [9] resulting in the penultimate effect, other called back strain effect [32, 33]: the radical similar to "MMA dimeric" species (obtained after one MMA addition onto EBiBr) is more stable than the first one derivated from EBiBr (Fig. 4). That leads to the preferential activation of the "dimer" compared to the activation of new initiator molecules. This effect could be exacerbated in DMSO where reaction is very fast, which would explain such no-quantitative efficiency (below 80%).

Influence of ligand: comparison of Bpy and n-Pr-PMI ligands

Influence of ligand is crucial in controlling ATRP. It enables metal catalyst solubilization but also modify its redox potential and thus its ability to abstract halogen from dormant species. The ligand effect on activation process has direct influence on ATRP kinetics constants, especially on the activation constant (k_{act}) [34]. To fully optimize activation step and ATRP control of MMA in DMSO, we thus compared the effect of some most known ligands to *n*-Pr-PMI, already been used for ATRP of MMA in polar solvents [34]. Best result was obtained with bipyridyne (Bpy) (Fig. 1) and that is the only result presented here (Fig. 2). Experimental conditions were chosen similar to the best one obtained with *n*-Pr-PMI: 60 °C, 10% molar ratio Cu(II)Br_2/Cu(I)Br initially added to fully optimize the polymerization and prevent persistent radical effect. A [Cu(I)]/[ligand] molar ratio

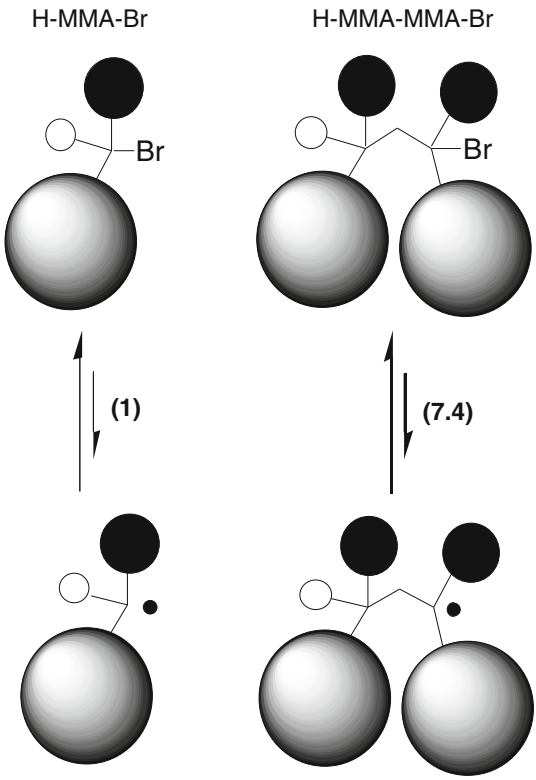

Fig. 4 Comparison of the relative values of the activation rate constants between "monomeric" dormant species H-MMA-Br (equivalent to EiBr), and "dimeric" dormant species H-MMA-MMA-Br. *Open circle* H, *filled circle* CH_3, *gray circle* $COOCH_3$. Relative values are given under *brackets* calculated from [32]

equal to 1:2, which is typical of bidentate ligand, was used to obtain the maximal values of k_{act}.

Compared to Bpy, *n*-Pr-PMI ligand exhibited slower polymerization rate but enabled a progressive consumption of the monomer over more than 300 min to reach 52% conversion. For comparison, 85% conversion was attained with Bpy in the same period, but the evolution of $\ln\left(\frac{[M]_0}{[M]_t}\right)$ was nearly linear until 40 min (50% conversion) then some downward curvature occurred. This decrease of polymerization rate in DMSO from Bpy to *n*-Pr-PMI is similar to previous results for polymerization in polar solvent [34]. For both ligands with an initial load of $Cu(II)Br_2$, both linear plots of $\ln\left(\frac{[M]_0}{[M]_t}\right)$ versus time (in accurate time scale) and SEC molecular weight versus theoretical ones, in addition with low polydispersities (below 1.2) confirmed the control of these polymerizations until at least 50% of conversion. Indeed, polymerization was controlled with Bpy on 40 min with an initiator efficiency (Eff) of 78%, while the control was observed all long the reaction (300 min) with *n*-Pr-PMI (Eff = 67%) (Table 1).

For both ligands, ATRP equilibrium constant can be evaluated from the kinetics data presented in Fig. 2. Actually, the evolution of $\ln\left(\frac{[M]_0}{[M]_t}\right)$ versus time and versus $t^{2/3}$ were linear, which meant than the initial $[Cu(II)Br_2]_0$ corresponds to the

Table 1 Experimental determination of apparent propagation rate and equilibrium constants (k_{app} and K_{eq}, respectively)

Ligand	k_{act} [a] (M^{-1} s^{-1})	k_{app} [b] (s^{-1})	K_{eq} [b]	Eff [b] (%)
n-Pr-PMI	2.4×10^{-3}	4.1×10^{-5}	1.8×10^{-7}	67
Bpy	6.6×10^{-2}	3.3×10^{-5}	1.3×10^{-6}/3.9×10^{-9}[c]	78

ATRP of MMA in DMSO at 60 °C with $[MMA]_0 = 4$ mol/L; $[MMA]_0/[EiBr]_0/[Cu(I)Br]_0/[Cu(II)Br_2]_0/[Ligand]_0 \approx 100/1/1/0.1/2$

[a,c] Values were measured using EBiBr as initiator and in the presence of Cu(I)Br/Ligand in acetonitrile at 35 °C and at 22 ± 2 °C, respectively [34, 39]

[b] Estimated from Fig. 2, for the ATRP of MMA in DMSO at 60 °C

($[Cu(II)Br_2]_{threshold}$) (as discussed above) and was sufficient to assume a near constant ratio of both $[Cu(II)Br_2]$ and [Cu(I)Br] throughout the polymerization [6, 7, 34], at least in the time range where $\ln\left(\frac{[M]_0}{[M]_t}\right)$ versus time remained linear. In addition, [Br], [Cu(I)], and [Cu(II)] should be close to their initial concentrations ($[Br]_0$, $[Cu(I)]_0$, and $[Cu(II)]_0$). Therefore, based on Matyjasweski's equation (Eq. 5), the slope of the kinetics semilogarithmic plot, that is the apparent propagation rate constant ($k_{app} = 3.26 \times 10^{-4}$ and 4.04×10^{-5} s^{-1} for Bpy and *n*-Pr-PMI, respectively, Table 1) can be related to the initial bromide concentration ($[Br]_0$) and to the initial copper molar ratio $\left(\frac{[Cu(II)]_0}{[Cu(I)]_0}\right)$:

$$\ln\left(\frac{[M]_0}{[M]_t}\right) = k_p K_{eq} \mathrm{Eff} \frac{[Br]_0[Cu(I)]_0}{[Cu(II)]_0} t = k_{app} \times t \quad (5)$$

where Eff is the initiator efficiency (here 0.67 or 0.78—see above) and $K_{eq} = \frac{k_{act}}{k_{deact}}$ with k_{act} and k_{deact}, the rate constants of activation and deactivation, respectively.

As already done by Matyjasweski et al. [6], the kinetics data from ATRP allow thus an estimation of equilibrium constant (K_{eq}) for ATRP of MMA in DMSO at 60 °C initiated by EBiBr with both ligands. Using available free radical propagation rate constants ($k_p = 833$ L mol^{-1} s^{-1} at 60 °C) [35, 36], K_{eq} values were finally calculated. Results are resumed in Table 1 and are of classical order of value for ATRP of MMA [6]. K_{ATRP} is seven times lower when *n*-Pr-PMI is used compared to Bpy. Thus, using *n*-Pr-PMI, the active species concentration is lower in the medium compared to Bpy. All of these results are in perfect agreement with k_{act} values obtained in another polar solvent like acetonitrile [34] (Table 1): k_{act} value of *n*-Pr-PMI is also considerably lower compared to Bpy (27 times lower). Moreover, one can notice for Bpy the very high value of K_{ATRP} in DMSO (1000 higher than value in acetronile). This comes from the catalytic effect of DMSO by complexation onto the metallic catalytic system, which enhance the polymerization. One can assume as already stated before that increase of K_{ATRP} is due to a k_{act} increase (k_{deact} decrease, respectively) with solvent polarity.

Grafting assays from macroinitiators

Based from the previous model study, ATRP of MMA can be controlled in DMSO by both ligands Bpy and *n*-Pr-PMI but Bpy giving far much faster polymerization compared to *n*-Pr-PMI, it is harder to use for accurate tuning of the conversion. That is why *n*-Pr-MI appeared as the preferable ligand in such a solvent for ATRP for MMA. Therefore, ATRP of MMA from dextran macroinitiators was performed with *n*-Pr-MI as ligand in similar conditions to those giving the best results with EBiBr, that is, at 60 °C with a initial load of low amount of Cu(II)Br_2 (10 molar % relative to Cu(I)Br).

On the one hand, assays on a protected macroinitiators DexAcBr gave controlled polymerization kinetics without gel formation until more than 50% of conversion. Some data are given in Table 2 for ATRP initiated from $DexAc_{71}Br_6$, which have already been published in detail [17]. PMMA grafts were analyzed after their deliberate cleavage from dextran backbone (see "Experimental section"). A linear increase of number average molecular weight of the grafts (obtained by SEC-MALLS) with conversion has been observed, while polydispersity indexes remains below 1.1. The comparison between experimental and theoretical $\overline{M_n}$ of PMMA grafts (calculated from conversion and $[MMA]_0/[Br]_0$ ratio) allowed us to evaluate an average grafting efficiency (Eff) of 53%, slightly lower to the value obtained with EBiBr as initiator model. Indeed, this grafting efficiency was the average efficiency for each initiator group carried by the polysaccharide chain.

On the other hand, all the first assays carried out in similar conditions from unprotected macroinitiators DexBr resulted in gel formation after only 30 min of polymerization (Fig. 5; Table 2). This gel formation was the result of intermolecular coupling between chains leading to cross-linking. Indeed, that is not really surprising as the polymerization was so quick in such conditions from DexBr, that

Table 2 Polymerization of MMA in DMSO at 60 °C from polysaccharidic macroinitiators

Used macroinitiator	$[MMA]_0/[Br]_0/[Cu^IBr]_0$ Molar ratio	Time (min)[a]	Conv.[b] (%)	M_n[c] (g/mol)	Ip[c]
$DexAc_{71}Br_6$	100/1/1	150	30	5,700	1.04
		240	42	7,800	1.04
		320	51	9,100	1.04
$DexBr_{5.6}$	97/1/1	30	91	*	*
	98/1/2	30	74	*	*
	100/1/2.5	30	15	5,800	1.68
		60	42	16,200	1.44
		135	80	37,700	1.17

Anisole/MMA = 1/10 (v:v); $[MMA]_0$ = 4 mol/L $[Cu(I)Br]_0/[Cu(II)Br_2]_0/[n\text{-Pr-PMI}]_0 \approx 1/0.1/2$ (molar ratio)

[a] Polymerization duration; [b] conversion yield determined by ^1H NMR (see "Experimental section"); [c] number average molecular weight and polydispersity index of the deliberately cleaved PMMA grafts (SEC–MALLS in THF, $dn/dc = 0.087$)

* At this conversion, an insoluble gel was formed

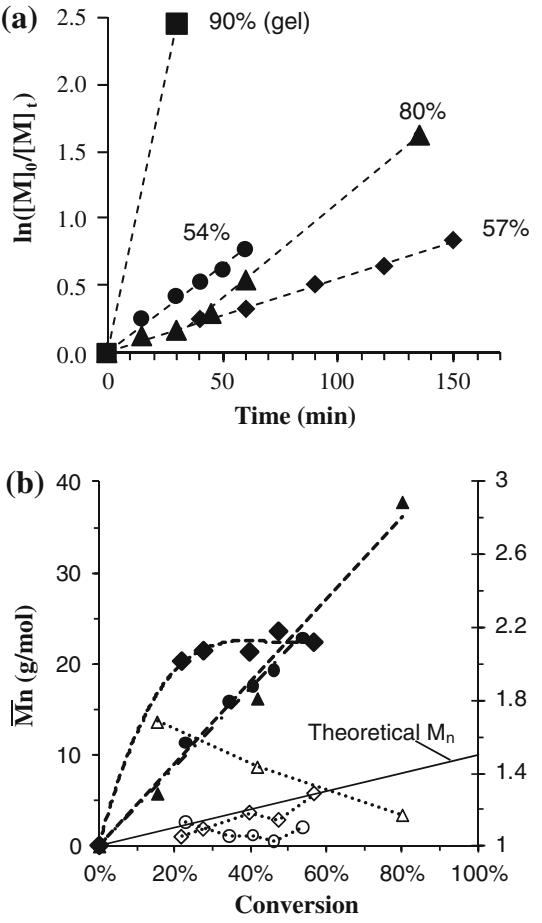

Fig. 5 Polymerization of MMA in DMSO using DexBr as macroinitiator. Anisole/MMA = 1/10 (v:v); $[MMA]_0 = 4$ mol/L; $[MMA]_0/[Br]_0 = 100/1$ and $[Cu(I)Br]_0/[Cu(II)Br_2]_0/[n\text{-Pr-PMI}]_0 = /1/0,1/2$ (molar ratio): **a** Evolution of $\ln([M_0]/[M_t])$ versus time. Maximum conversion is written for each experiment. **b** Evolutions of experimental $\overline{M_n}$ (*full symbols*), of theoretical $\overline{M_n}$ (*plain line*), and of polydispersity index I_P (*open symbols*, *dotted line*) versus conversion. With $[Br]_0/[Cu(I)Br]_0 = 1$ (molar ratio) *filled square*: from $DexBr_{5.6}$ at 60 °C (gel formation was observed); *filled circle*: from $DexBr_{4.3}$ at 45 °C; *filled diamond*: from $DexBr_{5.6}$ at 30 °C. With $[Br]_0/[Cu(I)Br]_0 = 2.5$ (molar ratio) *filled triangle*: from $DexBr_{5.6}$ at 60 °C

the local concentration of radicals was probably high in the vicinity of the backbone. Moreover, we assume that such a quick polymerization rate comes probably from the high-hydrophilic character of DexBr macroinitiator. In another "grafting from" strategy, Matyjaszewski et al. [37] have proposed to solve the problems of high concentration of radical growing chains by increasing the initial amount of cooper ($[Cu^IBr]_0$) compared to the initial initiator groups concentration ($[Br]_0$), while keeping constant Cu(II)/Cu(I) molar ratio. This is supposed to encourage chain deactivation and thus to reduce the window of time available for propagation. Therefore, occurrence of termination reaction should be decreased by reducing the period of time wherein growing chain are active. Even though polymerization rate of a controlled ATRP should theoretically not be reduced in this case, increasing $[Cu^IBr]_0/[Br]_0$ should delay or suppress gel formation and thus the increase of viscosity; so the increase of polymerization rate due to the increase of viscosity should also be attenuated or absent. Indeed, increasing $[Cu^IBr]_0/[Br]_0$ molar ratio to 2 reduces polymerization rate as conversion after 30 min is only of 74% instead of

90%, as presented in Table 2. Nevertheless, it is necessary to increase $[Cu^{I}Br]_0/[Br]_0$ molar ratio up to 2.5 to prevent gel formation. In this case, obtained kinetics curve depicted in Fig. 5a was linear up to a least 80% of conversion but a delay period of 20 min appeared which is common of ATRP polymerization with high amount of catalytic system. Another common way to increase the deactivation rate and thus prevent gel formation is to increase the initial amount of Cu(II) compared to Cu(I). Nevertheless, in our case, this method was inefficient even with high amount of $Cu(II)Br_2$ (such as 80 molar % relative to Cu(I)Br) as it induces large delay to the polymerization without preventing the loss of control and gel formation at the end. The last tested method to reduce radical amount was to decrease the temperature. Lower temperature decreases the ATRP equilibrium and thus favors deactivation compared to activation process [27, 38]. Instead of 60 °C, temperature was reduced to 45 and 30 °C. In both case, gel formation was prevented, and kinetics curves were linear up to more than 50% of conversion, as seen in Fig. 5a. At 45 °C, 54% of conversion was attained after only 60 min, while 150 min were necessary at 30 °C to get almost the same conversion.

To resume a linear kinetics curve could be obtained either by increasing the total amount of copper (up to $[Cu^{I}Br]_0/[Br]_0 = 2.5$) or by decreasing the temperature to 45 or 30 °C. To follow the evolution of the molecular mass distribution of the grafts, PMMA grafts were deliberately cleaved from dextran backbone then analyzed by SEC MALLS in THF. The M_n of the grafts and the corresponding polydispersity indexes are plotted versus conversion on Fig. 5b. At 30 °C, SEC chromatograms attested the presence of two populations even at low conversion (Fig. 6) and this phenomenon increased at higher conversion. In addition, the plot of M_n versus conversion was not linear for the kinetics at 30 °C and polydispersity indexes increases considerably with conversion. All of this attested the lack of control of the polymerization. As kinetics remained linear up to the studied conversion (57%), these results comes certainly from the occurrence of transfer reactions, which induces the early death of growing chains and formation of new chains. Furthermore, M_n are considerably higher than the theoretical ones due to low-initiator efficiency.

To the reverse, in the two others cases (polymerization at 45 or 60 °C with increased amount of copper), SEC chromatograms were very similar and presented only one population: chromatograms from the polymerization at 45 °C is given as example on Fig. 6 for comparison with the polymerization at 30 °C carried out with the same $[Cu^{I}Br]_0/[Br]_0$ molar ratio. Furthermore, M_n were also very similar in both cases and increased linearly with conversion. Polydispersities remained very low below 1.2 for polymerization at 45 °C, while they decreased from 1.8 to 1.2 with conversion for polymerization with higher amount of copper. In both these cases, linear plots $\ln\left(\frac{[M]_0}{[M]_t}\right)$ versus time and SEC molecular weight versus theoretical ones in addition with polydispersities confirmed the control of the polymerization until high conversion (80% for high-copper(I) load and 50% for polymerization at 45 °C) and attested the absence of noticeable transfer or combination reaction. Higher polydispersities with first polymerization carried out with high-copper load revealed a less perfect control compared to the second polymerization at 45 °C. Once again

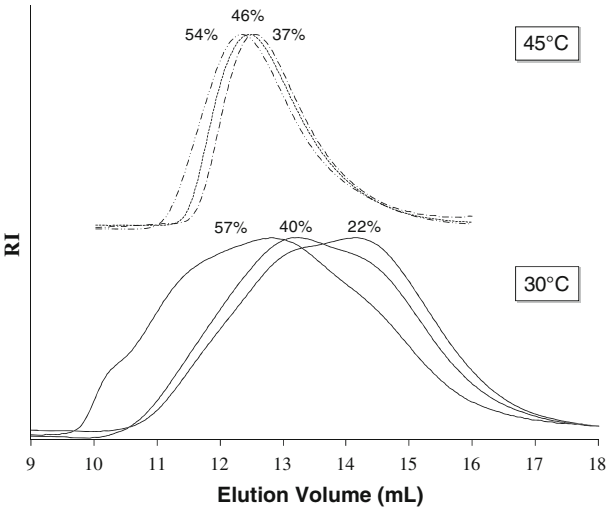

Fig. 6 Evolution of the SEC curves (THF, RI signal) of PMMA grafts produced from $DexBr_{5.6}$ at 45 °C (*upper curve*) and $DexBr_{4.3}$ at 30 °C (*bottom curve*) as function of conversion (written on the curve)

Table 3 Polymerization of MMA from DexBr in DMSO

Macroinitiator	Conversion in MMA (%)	PMMA grafts			Eff[c]
		Mn_{TH}[a] (g/mol)	Mn_{Exp}[b] (g/mol)	Ip[b]	
$DexBr_{5.6}$	15.4	1,550	5,800	1.68	0.22
	41.9	4,220	16,200	1.44	
	80.3	8,100	37,800	1.12	
$DexBr_{4.3}$	22.8	2,280	11,400	1.13	0.23
	34.5	3,450	15,900	1.06	
	40.7	4,070	17,600	1.06	
	46.2	4,630	19,400	1.03	
	53.7	5,370	22,800	1.10	

Anisole/MMA = 1/10 (v:v); $[MMA]_0 = 4$ mol/L

Conditions of synthesis: $DexBr_{5.6}$: 60 °C, $[MMA]_0/[Br]_0/[CuIBr]_0/[CuIIBr_2]_0/[n\text{-Pr-PMI}]_0 = 100/1/2.5/0.25/5$; $DexBr_{4.3}$: 45 °C, $[MMA]_0/[Br]_0/[CuIBr]_0/[CuIIBr_2]_0/[n\text{-Pr-PMI}]_0 = 100/1/1/0.1/2$

[a] Theoretical M_n calculated from conversion and $[MMA]_0/[Br]_0$ ratio

[b] Experimental M_n evaluated by SEC–MALLS in THF with $dn/dc = 0.087$

[c] Average efficacity evaluated by the ratio $M_{n_{Exp}}/M_{n_{Th}}$

the experimental $\overline{M_n}$ (obtained by SEC) are higher that the theoretical one (calculated from conversion and $[MMA]_0/[Br]_0$ ratio) due to initiator efficiency (Fig. 5b; Table 3). Whatever the experimental conditions (high-copper load at 60 °C or polymerization at 45 °C), an average grafting efficiency (Eff) could be evaluated around 23%.

Conclusion

ATRP of MMA in DMSO was reinvestigated to optimize its control in such a polar medium, in order to apply it to polymerization from hydrophilic dextran macroinitiator. ATRP was carried out at 60 °C, using [Cu(I)Br]/*n*-Pr-PMI as catalytic system and EBiBr as model initiator. Polymerization was quite fast and its control was delicate as a consequence of the great influence of "persistent radical effect" in such a medium. Contrary to previous reports, initial adding of low amount of $Cu(II)Br_2$ (10 molar % relative to Cu(I)Br) was necessary to obtain a controlled ATRP. Bpy was also proved to be efficient as ligand to control the ATRP of MMA in such experimental conditions. Nevertheless Bpy giving far much faster polymerization compared to *n*-Pr-PMI, *n*-Pr-PMI appeared as the preferable ligand in such a solvent for accurate tuning of the conversion and was chosen for polymerization from macroinitiators derivated from dextran.

Two types of macroinitiators were tested for polymerization of MMA in the determined conditions: protected DexAcBr, which have been protected by acetate group prior to initiator group introduction, and unprotected DexBr. The first type is less hydrophilic compared to the second. Conditions optimized with the model initiator were perfectly applicable for polymerization from protected DexAcBr macroinitators. To the reverse, polymerization was much faster in the same conditions from the unprotected macroinitiator leading to gel formation due to irreversible intermolecular termination reaction. Increasing the total amount of Cu(I)Br relative to initiator groups concentration or decreasing of polymerization temperature to 45 °C led to controlled polymerizations from DexBr. In these last cases, initiator efficiency is lower compared to homopolymerization. In the next future, we will compare both ATRP of MMA and the two strategic pathways using protected or unprotected macroinitiators in more details. This would give us a versatile method to prepare a wide range of comblike derivatives based on polysaccharide by ATRP in DMSO.

Acknowledgments The authors express their highest gratitude to Marie-Christine Grassiot for help in SEC measurements and Olivier Fabre for NMR measurements. Ludovic Dupayage was supported by a grant of the French Ministry in charge of Research.

References

1. Coessens V, Pintauer T, Matyjaszewski K (2001) Functional polymers by atom transfer radical polymerization. Prog Polym Sci 26:337–377
2. Matyjaszewski K, Xia J (2001) Atom transfer radical polymerization. Chem Rev 101:2921–2990
3. Kamigaito M, Ando T, Sawamoto M (2001) Metal-catalyzed living radical polymerization. Chem Rev 101:3689–3745
4. Borner HG, Matyjaszewski K (2002) Graft copolymers by atom transfer polymerization. Macromol Symp 177:1–15
5. Pyun J, Kowalewski T, Matyjaszewski K (2003) Synthesis of polymer brushes using atom transfer radical polymerization. Macromol Rapid Commun 24:1043–1059
6. Pyun J, Jia S, Kowalewski T et al (2003) Synthesis and characterization of organic/inorganic hybrid nanoparticles: kinetics of surface-initiated atom transfer radical polymerization and morphology of hybrid nanoparticle ultrathin films. Macromolecules 36:5094–5104

7. Zhang HQ, Klumperman B, Ming WH et al (2001) Effect of Cu(II) on the kinetics of the homogeneous atom transfer radical polymerization of methyl methacrylate. Macromolecules 34:6169–6173
8. Haddleton DM, Crossman MC, Dana BH et al (1999) Atom transfer polymerization of methyl methacrylate mediated by alkylpyridylmethanimine type ligands, copper(I) bromide, and alkyl halides in hydrocarbon solution. Macromolecules 32:2110–2119
9. Matyaszewski K, Wang J-L, Grimaud T et al (1998) Controlled/"Living" atom transfer radical polymerization of methyl methacrylate using various initiation systems. Macromolecules 31:1527–1534
10. Wang J-L, Grimaud T, Matyjaszewski K (1997) Kinetic study of the homogeneous atom transfer radical polymerization of methyl methacrylate. Macromolecules 30:6507–6512
11. Iovu M, Maithufi N, Mapolie S (2003) Copper-mediated ATRP of methyl methacrylate in polar solvents using a bifunctional pyridinal diimine ligand. Macromol Symp 193:209–226
12. Kimani SM, Moratti SC (2005) Ambient-temperature copper-catalyzed atom transfer radical polymerization of methacrylates in ethylene glycol solvents. J Polym Sci A 43:1588–1598
13. Iovu MC, Maithufi NG, Mapolie SF (2003) Evaluation of bis(2-pyridinal)ethylenediimine as ligand for atom transfer radical polymerization of methyl methacrylate: influence of polar solvents. Polym Int 52:899–907
14. Bontempo D, Masci G, De Leonardis P et al (2006) Versatile grafting of polysaccharides in homogeneous mild conditions by using atom transfer radical polymerization. Biomacromolecules 7:2154–2161
15. Wang J-S, Matyjaszewski K (1995) Controlled/"Living" radical polymerization. Halogen atom transfer radical polymerization promoted by a Cu(I)/Cu(II) redox process. Macromolecules 28:7901–7910
16. Yan L, Ishihara K (2008) Graft copolymerization of 2-methacryloyloxyethyl phosphorylcholine to cellulose in homogeneous media using atom transfer radical polymerization for providing new hemocompatible coating materials. J Polym Sci A 46:3306–3313
17. Dupayage L, Save M, Dellacherie E et al (2008) PMMA-grafted dextran glycopolymers by atom transfer radical polymerization. J Polym Sci A 46:7606–7620
18. Cai Y, Hartenstein M, Mueller AHE (2004) Synthesis of amphiphilic graft copolymers of *n*-butyl acrylate and acrylic acid by atom transfer radical copolymerization of macromonomers. Macromolecules 37:7484–7490
19. Nouvel C, Ydens I, Degée P et al (2004) Amphiphilic totally biodegradable copolymers grafted polylactide-grafted dextrans: controlled synthesis. J Polym Sci A 42:2577–2588
20. Nouvel C, Frochot C, Sadtler V et al (2004) Polylactide-grafted dextrans: synthesis and properties at interfaces and in solution. Macromolecules 37:4981–4988
21. Raynaud J, Choquenet B, Marie E et al (2008) Emulsifying properties of biodegradable polylactide-grafted dextran copolymers. Biomacromolecules 9:1014–1021
22. Nouvel C, Raynaud J, Marie E et al (2009) Biodegradable nanoparticles made from polylactide-grafted dextran copolymers. J Colloid Interface Sci 330:337–343
23. Sui X, Yuan J, Zhou M et al (2008) Synthesis of cellulose-graft-poly(*N*,*N*-dimethylamino-2-ethyl methacrylate) copolymers via homogeneous ATRP and their aggregates in aqueous media. Biomacromolecules 9:2615–2620
24. Meng T, Gao X, Zhang J et al (2009) Graft copolymers prepared by atom transfer radical polymerization (ATRP) from cellulose. Polymer 50:447–454
25. Lin C-X, Zhan H-Y, Liu M-H et al (2009) Preparation of cellulose graft poly(methyl methacrylate) copolymers by atom transfer radical polymerization in an ionic liquid. Carbohydr Polym 78:432–438
26. Patrizi ML, Piantanida G, Coluzza C et al (2009) ATRP synthesis and association properties of temperature responsive dextran copolymers grafted with poly(*N*-isopropylacrylamide). Eur Polym J 45:2779–2787
27. Monge S, Darcos V, Haddleton DM (2004) Effect of DMSO used as solvent in copper mediated living radical polymerization. J Polym Sci A 42:6299–6308
28. Ohno K, Wong B, Haddleton DM (2001) Synthesis of well-defined cyclodextrin-core star polymers. J Polym Sci A 39:2206–2214
29. Fischer H (1999) The persistent radical effect in controlled radical polymerizations. J Polym Sci A 37:1885–1901
30. Keller RN, Wycoff HD (1947) Copper(I) chloride. Inorg Synth 2:1

31. Mittal A, Sivaram S (2005) A novel tridentate nitrogen donor as ligand in copper catalyzed ATRP of methyl methacrylate. J Polym Sci A 43:4996–5008
32. Nanda AK, Matyjaszewski K (2003) Effect of penultimate unit on the activation process in ATRP. Macromolecules 36:8222–8224
33. Lin CY, Coote ML, Petit A et al (2007) Ab initio study of the penultimate effect for the ATRP activation step using propylene, methyl acrylate, and methyl methacrylate monomers. Macromolecules 40:5985–5994
34. Tang W, Matyjaszewski K (2006) Effect of ligand structure on activation rate constants in ATRP. Macromolecules 39:4953–4959
35. Beuermann S, Buback M (2002) Rate coefficients of free-radical polymerization deduced from pulsed laser experiments. Prog Polym Sci 27:191–254
36. Van Herk AM (2000) Pulsed initiation polymerization as a means of obtaining propagation rate coefficients in free-radical polymerizations. II. Review up to 2000. Macromol Theor Simul 9:433–441
37. Sumerlin BS, Neugebauer D, Matyjaszewski K (2005) Initiation efficiency in the synthesis of molecular brushes by grafting from via atom transfer radical polymerization. Macromolecules 38:702–708
38. Matyjaszewski K, Xia J (2006) Fundamentals of atom transfer radical polymerization. In: Matyaszewski K, Davis TP (eds) Handbook of radical polymerization. Wiley & Sons, New York
39. Tang W, Tsarevsky NV, Matyjaszewski K (2006) Determination of equilibrium constants for atom transfer radical polymerization. J Am Chem Soc 128:1598–1604